18TH WORLD CONFERENCE ON EARTHQUAKE ENGINEERING
WCEE2024
MILAN

MILAN, ITALY
30TH JUNE - 5TH JULY 2024
www.wcee2024.it

REAL TIME HYBRID SIMULATION (RTHS) OF A 2-STORY BUILDING EQUIPPED WITH NOVEL BASE ISOLATION SYSTEMS

Liang Cao[1], Faisal Nissar Malik[2], Safwan Al-Subaihawi[2], Wendy Miao[3], James Ricles[2], Thomas M Marullo[2], Chinmoy Kolay[4], Austin Downey[5] & Simon Laflamme[6]

[1] Lehigh University, Bethlehem, Pennsylvania, USA, lic418@lehigh.edu

[2] Lehigh University, Bethlehem, Pennsylvania, USA

[3] University of California San Diego, San Diego, California, USA

[4] Indian Institute of Technology Kanpur, Kanpur, India

[5] University of South Carolina, Columbia, South Carolina, USA

[6] Iowa State University, Ames, Iowa, USA

Abstract: *A new friction device using band brake technology, termed the Banded Rotary Friction Damper (BRFD), has been fabricated at the NHERI Lehigh Experimental Facility. The damping mechanism is based on band brake technology and leverages a self-energizing mechanism to produce large damping forces with low input energy. The device is a second-generation BRFD, where the friction mechanism is achieved using two electric actuators. The BRFD generates a damping force as a function of the input force provided by the electric actuators, where the ratio of BRFD force output-to-electric actuator force input is equal to about 112. The paper presents the results of a study using real-time hybrid simulations (RTHS) to investigate the performance of the BRFD's in mitigating seismic hazards of a two-story reinforced concrete building. The building has two and three special moment resisting frames (SMRFs) in the east-west and north-south directions, respectively. In order to perform the RTHS, the north south SMRF is considered and the BRFD along with a parallel elastic member is used as a base isolation system to mitigate the effects of earthquake hazards by reducing story drift and floor accelerations of the structure. For the RTHS the building and the elastic component of the isolator are part of the analytical substructure while the experimental substructure is comprised of the BRFD. The response of the structure is investigated involving six Maximum Considered Earthquake (MCE) hazard level events that includes three near-field and three far-field ground motions. The explicit, unconditionally stable dissipative Modified KR-α integration algorithm is used to accurately integrate the equations of motion during the RTHS. The model for the reinforced concrete building is created using explicit non-linear force-based fiber elements to discretely model each member of the structure. First, the details of the prototype of the BRFD are presented. Second, the details of the isolator system consisting of a linear spring element and the BRFD are discussed. Finally, the details of the RTHS study and the results are presented. The building's inter-story peak and residual story drift from base-isolated and fixed-based conditions are compared. Results show that the proposed isolator system produces a significant reduction in both maximum inter-story drift and residual drift, and reduces the damage developed in the structure during the MCE.*

1. Introduction

Civil infrastructures such as buildings, lifelines, energy, and transportation systems are keystones in communities. These systems need to be designed and maintained to ensure daily operability and public safety.

However, when the civil infrastructure is subjected to extreme natural hazard events such as earthquakes the structures of this infrastructure are susceptible to damage, increasing the likelihood of structural failure and downtime.

A solution to improve structural performance vis-a-vis seismic loads is to integrate base isolation systems into the structure in order to mitigate structural vibrations, dissipate earthquake energy, and minimize the amount of energy absorbed and damage developed in the structure. Decoupling the structural and isolator vibrations during earthquakes leads to displacements and yielding becoming concentrated in the base isolation system, enabling the structure to act as a rigid body (Deb 2004). Isolated structures exhibit an increase in their fundamental period and become less susceptible to high-frequency accelerations (Jangid and Kelly 2001).

The sliding type of base isolation systems, such as the Friction Pendulum System (FPS) and Double Concave Friction Pendulum system (DCFP), provide re-centering characteristics that can restore base isolation systems to their initial position after earthquakes (Montazeri et al. 2023). However, these systems have limited energy dissipation capability and do not perform well against near-field earthquakes since the impact typically comes in the form of a shock and not a build-up of energy (Cao et al. 2014). In addition, FPS and DCFP rely on the weight of the building to impose the normal force to produce the friction force in the isolation system. As a result, these structures are susceptible to the effects of ground motion's vertical accelerations, where upward accelerations can cause the frictional force to be too high and subsequently lead to structural damage, and downward accelerations cause the normal force to be reduced or lost, leading to excessive isolator deformations and a likelihood of impacting the moat after exceeding the stroke limit of the isolation system.

To cope with the susceptibility of FPS and DCFP to vertical accelerations, the authors proposed a new type of friction device, termed Banded Rotary Friction Device (BRFD), which can substantially enhance structural performance under multiple hazards (Downey et al. 2016, Huggins et al. 2023). The mechanical principle of the BRFD is based on existing band brake technology, constituting a mechanically reliable mechanism. Two electric actuators are used to achieve the friction mechanism. To assess the efficacy of a BRFD in mitigating the damaging effects of a seismic hazard to a structural system, real-time hybrid simulations (RTHS) are used to assess the Maximum Considered Earthquake (MCE) seismic performance of a two-story isolated reinforced concrete building outfitted with a BRFD base isolation system. The MCE has a 2% of exceedance in 50 years (2475 return year period). The BRFD along with linear spring elements are used as the base isolation system. RTHS is a cost-effective method for performing experimental validation of natural hazard mitigation strategies, where most of the structural system is modeled numerically in the computer as the analytical substructure and only a portion of the structure is physically present in the laboratory as the experimental substructure. For the RTHS study in this paper, the building and the linear spring component of the isolator system are part of the analytical substructure while the BRFD forms the experimental substructure. Six MCE-level earthquakes are considered including three near-field and three far-field ground motions. The explicit, unconditionally stable dissipative Modified KR-α integration algorithm is used to accurately integrate the equations of motion during the RTHS (Kolay and Ricles 2019). The model for the reinforced concrete building is created using explicit non-linear force-based fiber elements to discretely model each member of the structure (Kolay and Ricles 2018).

The remaining part of the paper is organized as follows. The next section describes a detailed background of the BRFD and presents its hysteretic behavior. The subsequent section presents the RTHS study on the two-story isolated reinforced concrete building and discusses the results. The last section provides a summary and the conclusions of the study.

2. Banded rotary friction device

The Banded Rotary Friction Damper (BRFD is a variable friction damper based on existing reliable band brake technology. The BRFD consists of three steel bands lined with a ceramic friction material that are wrapped around a cylindrical steel drum. During excitation the drum rotates, and contact pressure between the drum and bands increases that substantially amplifies the output friction force. This phenomenon, termed as a self-energizing mechanism, is able to produce large friction capacity using low energy input. The friction mechanism is achieved using two electric actuators for the purpose of applying tension force onto the steel bands and controlling the normal force on the drum surface.

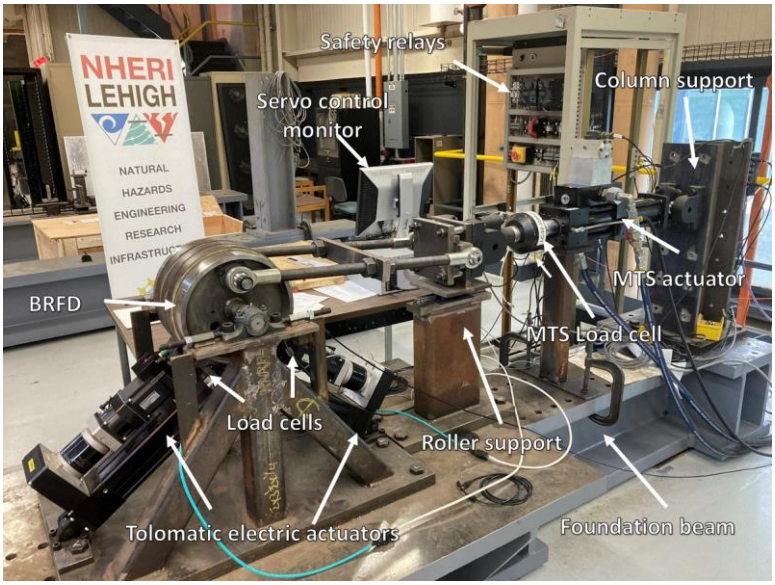

Figure 1: Experimental test setup of the BRFD at the NHERI Lehigh Experimental Facility.

A second-generation BRFD was fabricated and its dynamic behaviour was characterized at the NHERI Lehigh Real-Time Cyber-Physical Structural Systems Laboratory (Cao et al. 2020). The test setup is shown in Figure 1. In the test setup the BRFD was installed on a foundation beam and connected to an MTS actuator via a clevis. The actuator's displacement was controlled through a servo-hydraulic control system and the BRFD's output force was measured by the actuator load cell. The BRFD input force was applied by the electric actuators using a closed-loop PID control system, and the force of each actuator was measured using load cells connected with the electric actuators.

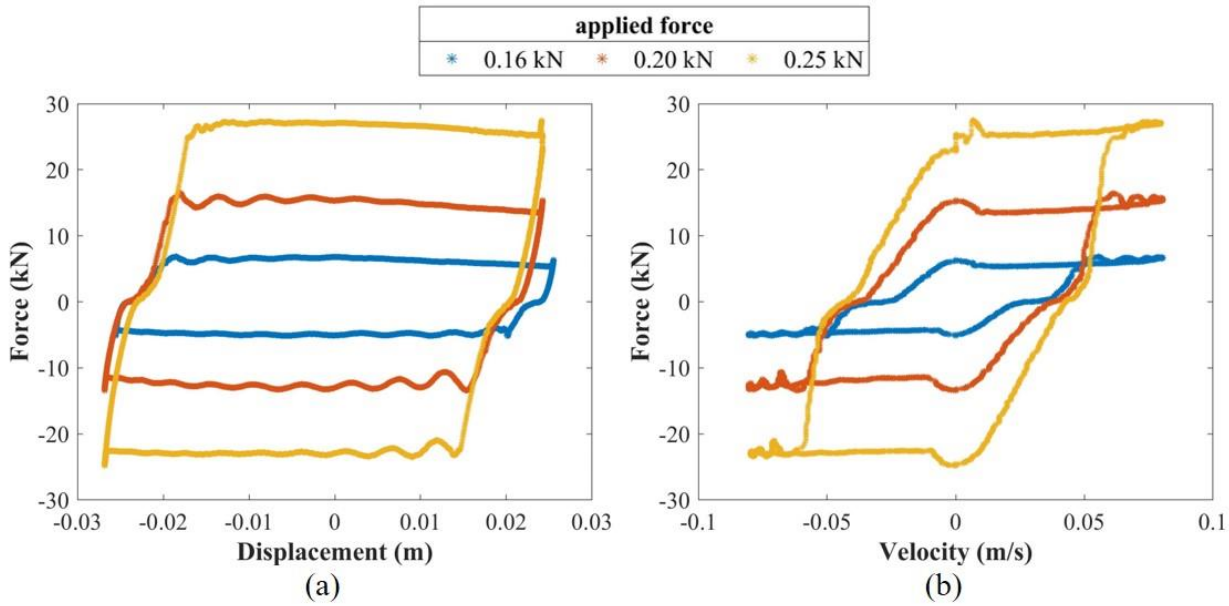

Figure 2: Characterization tests of BRFD under harmonic testing at 0.5 Hz: (a) damper force-displacement hysteretic response, and (b) damper force-velocity hysteretic response.

To conduct the characterization test, the BRFD was subjected to a history of displacement-controlled harmonic excitation having a 25.4 mm amplitude with a frequency of 0.5 Hz. Three different values of constant applied force from the electric actuators were investigated and included 0.16, 0.2, and 0.25 kN. The force-displacement and force-velocity response of the BRFD are plotted in Figure 2. The results show that the BRFD is capable of obtaining a maximum damping force of 28 kN when using an applied tension force to the bands of 0.25 kN,

resulting in a maximum force amplification ratio (FAR) of 112. The FAR is defined as the ratio of BRFD force output to electric actuator force input.

3. Seismic mitigation application example: RTHS of two-story BRFD base-isolated reinforced concrete building

3.1 Prototype structure

The prototype structure used for validating the seismic hazard mitigation effectiveness of the BRFD as part of a base isolation system is a 2-story reinforced concrete frame adapted from Kolay and Ricles (2018). The building was assumed to be located in Los Angeles, California. The plan and elevation of the building are shown in Figure 3. The prototype building is designed in accordance with ASCE 7-10 (ASCE, 2010), where the columns and beams are designed and detailed per ACI 318-11 (ACI, 2011). The member reinforcement details are given in Figure 4.

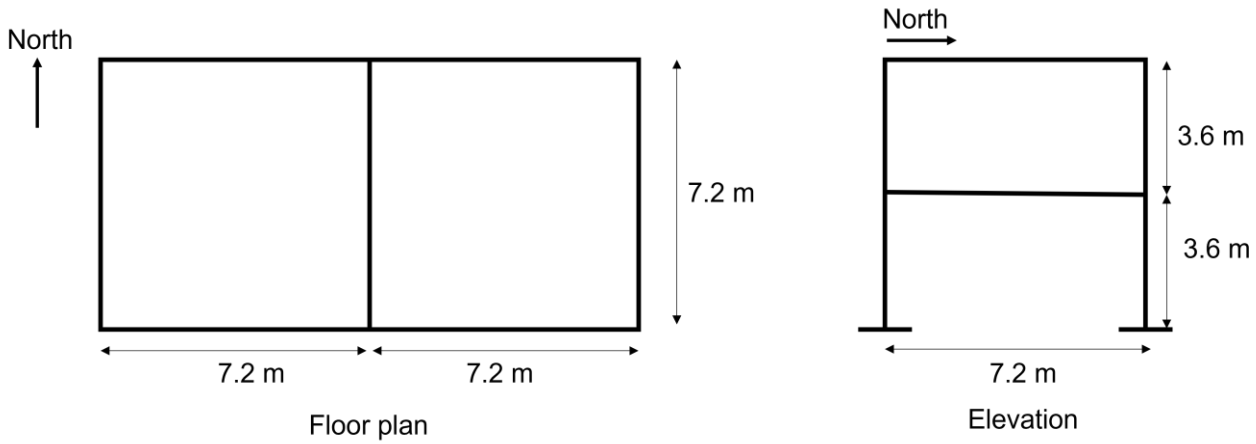

Figure 3: The floor plan and the elevation of the prototype structure.

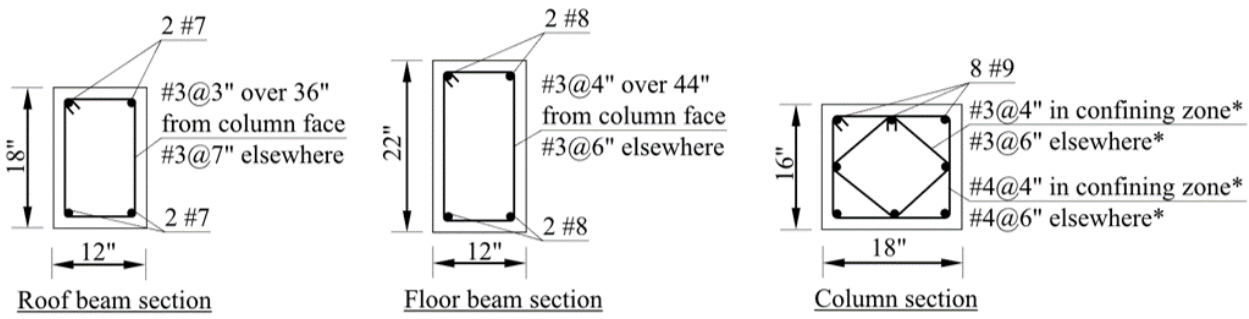

* Column confining zones measure 22" from the face of the beams and 33" from the base of the column

Figure 4: The detailing of the columns and beams (Ricles and Kolay (2018)); note: 1 inch = 25.4 mm.

To cope with the stroke limit of the BRFD as the experimental substructure, a one-tenth reduced scale finite element model was developed in HyCOM-3D (Ricles et. al (2020)), a multi-hazard 3D non-linear structural system response simulation program, as shown in Figure 5. The scaled finite element model was used as the analytical substructure for the RTHS. The beams and columns were modeled using explicit force-based fiber-elements (Kolay and Ricles (2018)). Each story column was modeled by one element, and the beams in north-south and east-west directions were modeled using two elements. The sections were modeled as reinforced concrete sections with 10 fibers in the core and 5 fibers in the cover. The structure had a total of 40 force-based fiber elements. The floor masses were lumped at the master-node on each floor. Rigid floor diaphragms were used to slave floor nodes to the master node. $P-\Delta$ effects were considered by using a lean-on column as shown in Figure 5, which modeled the gravity frame system of the building. Due to the availability of only one BRFD, the structure is analyzed in the north-south direction only, as shown in Figure 3.

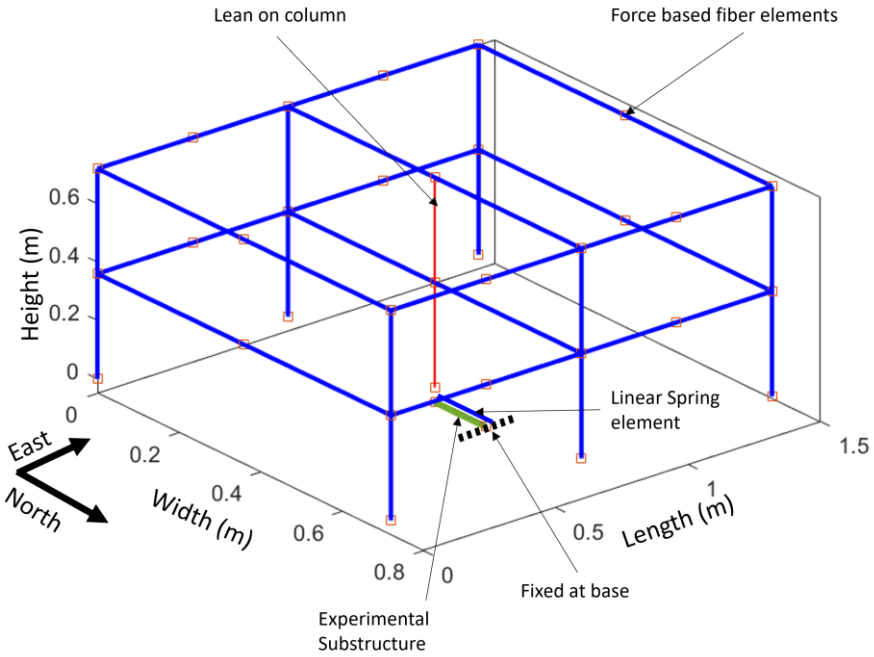

Figure 5: Analytical substructure finite element model of the building showing the nodes, fiber-elements, and lean-on column (experimental substructure shown for completeness).

3.2 Selection and scaling of ground motion records

To evaluate the performance of the base isolation system a suite of ground motions was selected and scaled to match a target spectrum. The target spectrum is the MCE hazard level spectrum defined in accordance with ASCE 7-22 (ASCE, 2022) for Los Angeles, California with soil type D. The S_{Ds} and S_{D1} values for the design spectrum are 1.52 g and 1.11 g, respectively, and the MCE level spectrum is 1.5 times the design spectrum. The MCE event has a probability of exceedance of 2% in 50 years. S_{Ds} and S_{D1} for the MCE are defined as the spectral accelerations at short periods and at a period of 1 sec (ASCE, 2022). The ensemble of ground motions consisted of three far-field and three near-field ground motions that were downloaded from the PEER NGA West 2 database (Ancheta et al., 2013). Since the prototype structure is analyzed in one direction, only one component of the ground motions is used. The records were scaled to match the target spectrum where the scale factor for each record is obtained by minimizing the weighted sum of the squared errors between the target spectrum and the acceleration spectrum for a ground motion. 90% weights are assigned to errors in the period range of 0.08 sec to 2 sec and a 10% weight is assigned to errors in the period range of 2 sec to 5 sec, where the error is the difference between the acceleration spectrum and the target spectrum. The target spectrum, the median spectrum, and the $\mu \pm \sigma$ spectrum are shown in Figure 6, where μ and σ are the mean and standard deviation, respectively. The ground motions and the scale factors are tabulated in Table 1. The details of the record scaling procedure is given in Malik and Kolay (2023).

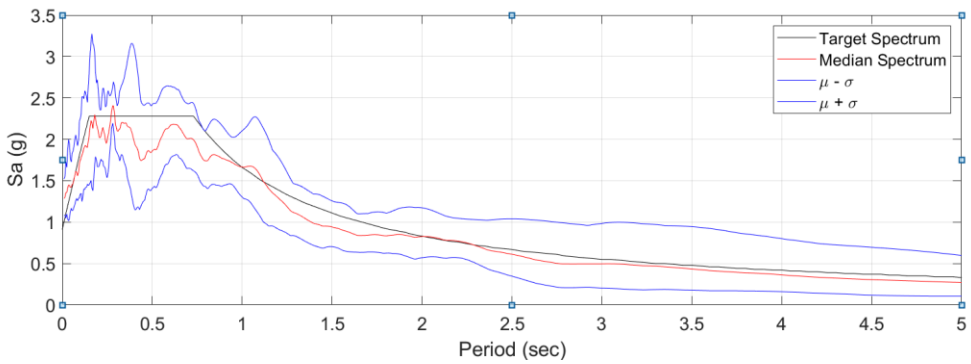

Figure 6: The median and target spectrum for the considered location of the building.

Table 1: Ground motion ensemble used for the study.

Ground motion (GM)	Earthquake name	Year	Type	Recording station	Component	Scale factor
1	Kocaleli	1999	Far-field	Duzce	180	3.39
2	ChiChi	1999	Far-field	CHY101	East	3.48
3	ChiChi	1999	Near-field	TCU065	East	1.71
4	Imperial Valley	1979	Near-field	El Centro Array #7	E07140	3.27
5	Loma Prieta	1989	Near-field	Saratoga-Aloha Ave	000	3.07
6	ChiChi	1999	Far-field	TCU045	North	2.99

3.3 Isolation system design procedure

The proposed base isolation system consists of the BRFD and a parallel linear elastic member, as shown in Figure 7, where d represents the isolator displacement, k the elastic member's stiffness and f the damping force of the BRFD. The BRFD depicts a controllable damping force and the elastic member provides a minimal isolation stiffness when the BRFD is in a fail-safe mechanism state. The equivalent lateral force procedure from Chapter 17 in ASCE 7-22 (ASCE, 2022) is used to design the isolator components, including the elastic member's stiffness k and the BRFD required damping force output f.

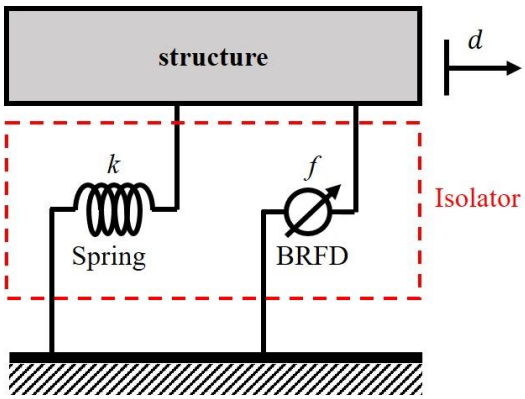

Figure 7: Simplified diagram of BRFD isolation system.

The design of the isolator used in the two-story isolated reinforced concrete building consist of the following steps:

1. Assume the effective period of the isolated structure T_D, and the isolator design displacement d_D.
2. Calculate the effective stiffness of the isolator system, k_{eff},

$$k_{eff} = \frac{4\pi^2}{T_D^2}\frac{\mathrm{W}}{\mathrm{g}} \quad (1)$$

   where W is the effective seismic weight of the structure above the isolator and g the acceleration of gravity.
3. Assume the effective damping ratio of the isolator β_D and determine the required design damping capacity of the BRFD using the equivalent energy dissipation concept (Chopra, 2011),

$$f = \frac{\beta_D \pi k_{eff} d_D}{2} \quad (2)$$

4. Determine the stiffness of the elastic element,

$$k = k_{eff} - \frac{f}{d_D} \quad (3)$$

5. Calculate the peak dynamic displacement d_p of the isolation system using the design response spectrum,

$$d_p = \frac{S_{D1} g\, T_D}{4\pi^2 B_M} \quad (4)$$

where B_M is the damping factor based on the effective damping of β_D from Table 17.5-1 in ASCE 7-22, and S_{D1} the design 5 percent damped spectral acceleration parameter at a period of 1 sec.

6. Repeat the design process from step 3 until the design displacement d_D and calculated peak dynamic displacement d_p become almost equal; setting d_D equal to d_p at the start of each repetition.

The parameter values of the full-scale base isolation system determined from the above design procedure are summarized below in Table 2. After iteration, the peak dynamic displacement response d_p is close to the design displacement d_D which indicates that the design is complete. Note that the design displacement d_D must be within the stroke capacity of the full-scale BRFD.

Table 2. Isolator parameter values (full-scale).

Parameter	**Symbol**	**Value**
Effective period	T_D	3 sec
Effective stiffness	k_{eff}	1659.9 kN/m
Effective damping ratio	β_D	30%
Damping coefficient	B_M	1.7
Spring stiffness	k	906 kN/m
BRFD damping force	f	377 kN
Design displacement	d_D	0.5 m
Peak dynamic displacement response	d_p	0.496 m

3.4 RTHS configuration

The RTHS configuration for the 2-story isolated reinforced concrete building is shown in Figure 8. The 1:10 scaled model of the 3D RC building and linear spring element of the isolator system are incorporated into the analytical substructure while the remaining BRFD in the isolator is modelled physically in the laboratory as the experimental substructure. Since the BRFD is able to deform only in a unidirectional manner, the degrees of freedom of the analytical substructure associated with motion in the east-west (EW) direction are restrained and the earthquake ground accelerations are applied in the NS direction of the structure. By solving the equations of motion in real-time, the command displacements are calculated by the integration algorithm and imposed onto the experimental and analytical substructures. After receiving the feedback restoring forces from these substructures, the simulation coordinator completes the integration of the equations of motion and the process is repeated for each subsequent time step. As mentioned above, the unconditionally stable explicit Modified KR-α method was used to integrate the equations of motion. The integration time step was selected as Δt = 6/1024 sec. Since the RTHS were conducted using a model at 1:10 scale, the time axis was compressed by the square root of the scale factor of $\sqrt{1/10}$ from the full-scale model simulation time step Δt

= 19/1024 sec to maintain modelling similitude. The RTHS used the same test setup for the experimental substructure as that of the characterization tests. The adaptive times series (ATS) compensator (Chae et al., 2013) was used to ensure accurate actuator control when imposing displacements to the experimental substructure.

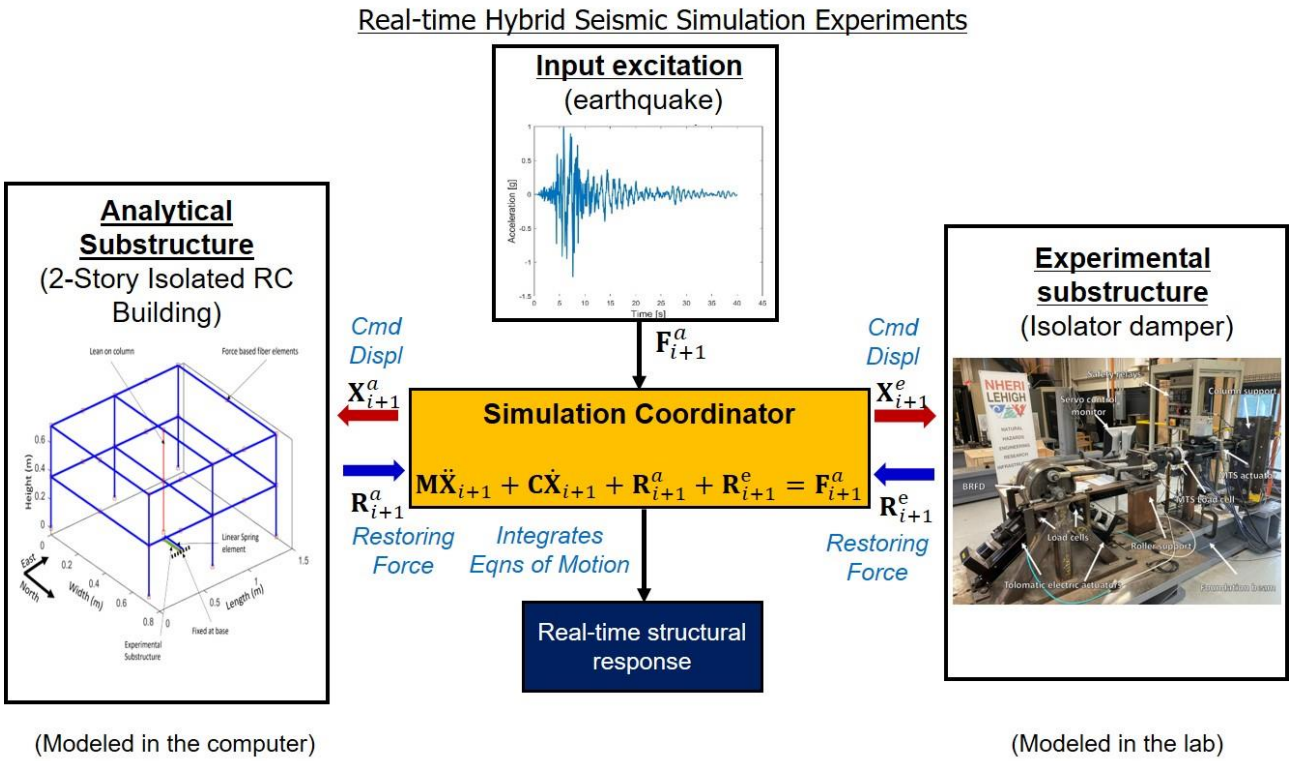

Figure 8: Schematic of real-time hybrid seismic simulation of a base-isolated 2-story reinforced concrete building.

3.5 Results and discussion

This section presents the RTHS results of the base-isolated structure and a comparison with the case when no base isolation was used (called the fixed-based structure). Figure 9 shows the synchronization subspace plots from the RTHS for the Loma Prieta earthquake (GM5). As can be seen in Figure 9, the target and measured displacement for the actuator match closely, with a normalized root mean square error (NRMSE) of 0.21% indicating superior actuator control with the use of the ATS compensation scheme. These results are representative of the NRMSE for the other five RTHS. Note that the NRMSE is defined as follows:

$$NRMSE = \frac{\sqrt{\frac{1}{N}\sum_{i=1}^{N}(d^{measured}(i) - d^{target}(i))^2}}{\max(\boldsymbol{d}^{target}) - \min(\boldsymbol{d}^{target})} \times 100 \quad (5)$$

In Equation (5) $d^{measured}$ and d^{target} are the measured and target actuator displacements and N is the length of the time series.

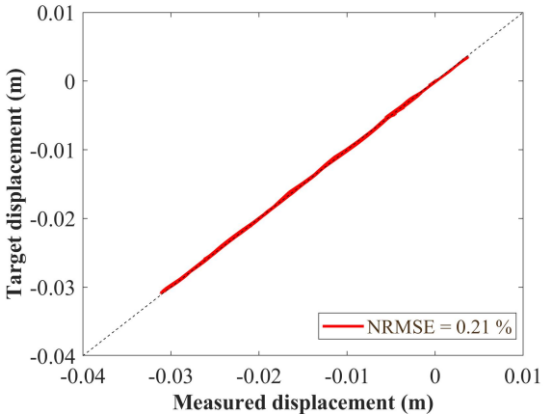

Figure 9: Synchronization subspace plot for actuator motion; RTHS using near-field Loma Prieta EQ (GM5).

The time history of the inter-story drift response to the near-field Loma Prieta ground motion (GM5) is presented in Figure 10. The statistics for the remaining RTHS involving the other ground motions are discussed later. As can be seen in Figure 10, the peak inter-story drifts of the base-isolated structure are significantly reduced in comparison to that of the fixed-base structure. The results show that the base-isolated structure has minimal damage where the peak inter-story drifts are less than 2% and the residual inter-story drifts are less than 0.25% in the two stories. The fixed-base structure has peak inter-story drifts close to 6% and residual inter-story drifts around 1%. This implies that the structure without base isolation suffers permanent damage and needs to be rehabilitated if it is susceptible to an earthquake at the MCE intensity. The moment-curvature relationship at the base of the 1st story column and at the ends of the floor and roof beams for the same ground motion are shown plotted at full-scale in Figure 11. The figure shows that the flexural capacity has been reached with the formation of plastic hinges, followed by a deterioration in the strength with pinching in the hysteretic response at the base of the 1st story columns as well as the 1st floor and roof beams. On the other hand, the base-isolated structure demonstrates a significant reduction in the curvature and ductility demand on the beams and columns, thereby indicating the efficacy of the proposed base isolation system in reducing damage. The full-scale force-displacement hysteretic behavior of the BRFD under the near-field Loma Prieta ground motion (GM5) is plotted in Figure 12. The BRFD behavior exhibits a sudden drop in resistance when the force undergoes a change in sign due to the backlash effect. The backlash phenomenon is difficult to analytically model, suggesting the importance of performing RTHS where these devices are modelled physically in the laboratory as part of the experimental substructure.

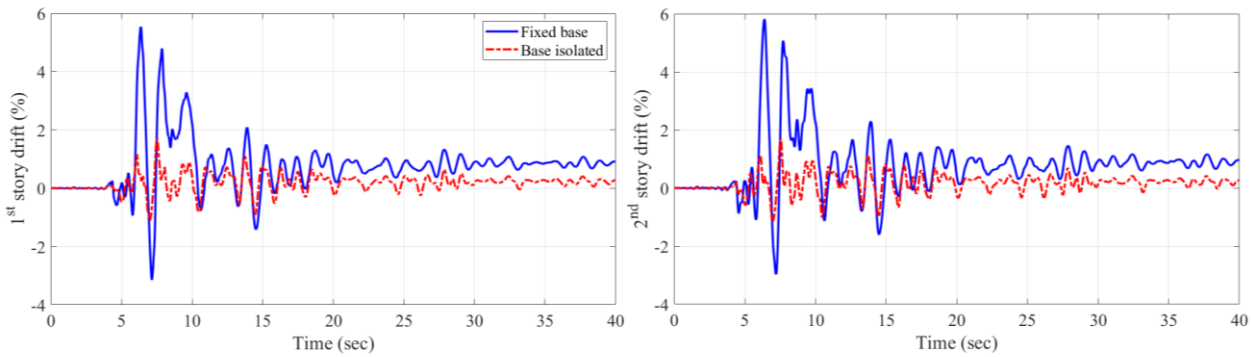

Figure 10: Residual and peak story drifts of base-isolated and fixed-base structures; near-field Loma Prieta ground motion (GM5)

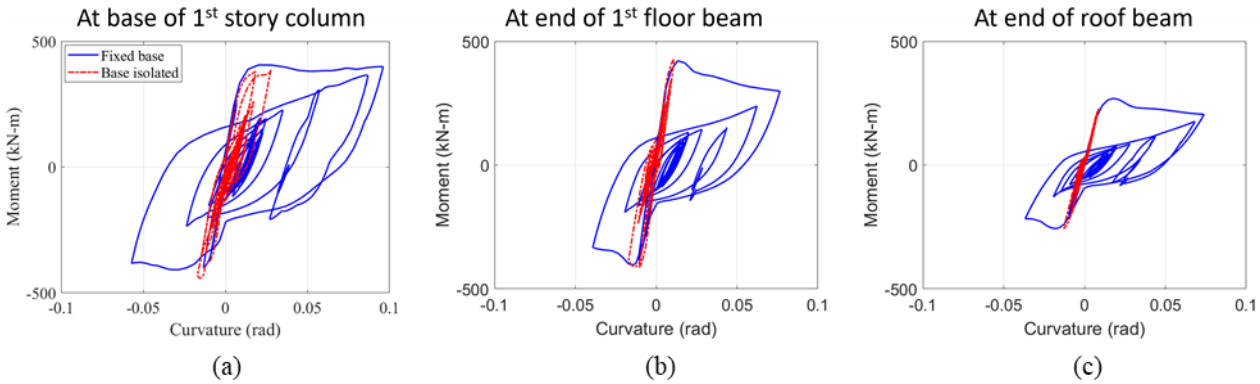

Figure 11: Moment curvature relationship at (a) base of 1st story column, and at the ends of (b) floor and (c) roof beams of base-isolated and fixed-based structures; near-field Loma Prieta ground motion (GM5).

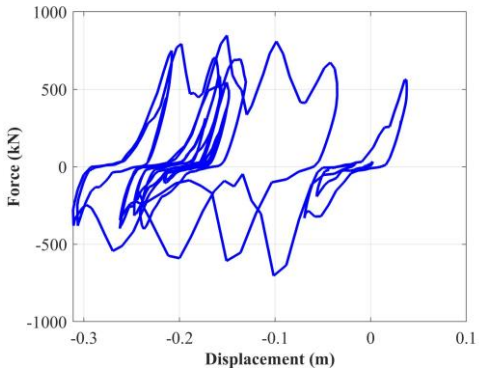

Figure 12: Hysteretic behavior of BRFD base isolator; near-field Loma Prieta ground motion (GM5).

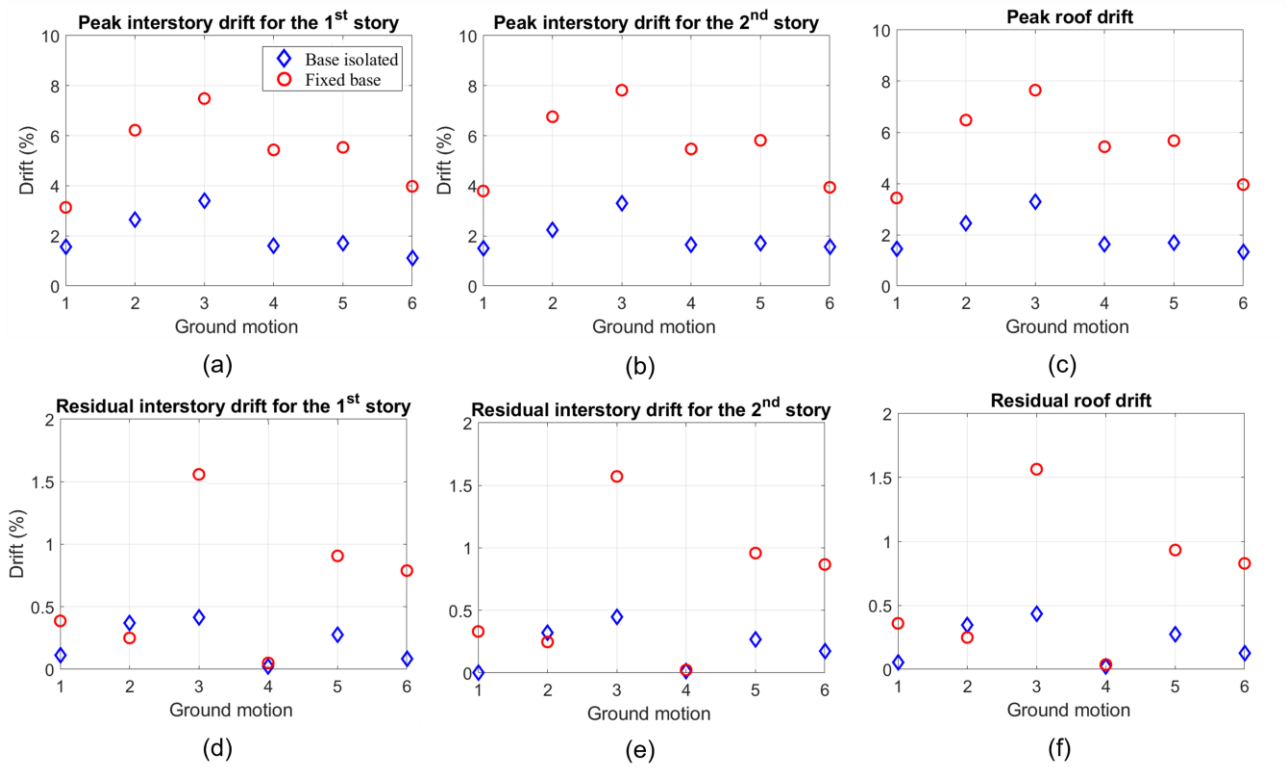

Figure 13: Peak and residual story drifts for the six considered ground motion records.

Figure 13 compares the peak and residual inter-story drifts for the 1st and 2nd stories as well as the roof drift of the base-isolated and fixed-base structures for the ensemble of ground motions. The roof drift is defined as the relative displacement between the roof and isolator divided by the height from the top of the isolator to the roof of the structure. As shown in the Figure 13, the peak and residual drifts are significantly reduced when the structure is equipped with the base isolation system. For the most demanding earthquake (ChiChi EQ recorded at station TCU065 - GM3) the peak drifts of the fixed-based structure are about 8% whereas that for the base-isolated structure are reduced to about 3.5%. For the same ground motion, the maximum residual drifts in both stories and the roof drift are reduced to less than 0.5% in the base-isolated structure compared to about 1.5% for the fixed-base structure. Hence, the base isolation system shows a reduction of 56% in the peak drifts and a reduction of about 66% in the residual drift for this ground motion. The percentage reduction of the median peak and the residual inter-story and roof drifts for the six ground motions are summarized in Table 3. The reduction in the medium of the peak roof drift is 70.1%, with the reduction in the 1st story and 2nd story medium peak drift equal to 70.1% and 70.4%, respectively. The reduction in the medium residual roof drift is 66.3%, with the 1st and 2nd stories having a reduction of 34.3% and 50.8%, respectively.

Table 3: Reduction in median of peak and residual story drift.

Peak roof drift	Peak 1st story drift	Peak 2nd story drift	Residual Roof drift	1st story residual drift	2nd story residual drift
70.1%	70.1%	70.4%	66.3%	34.3%	50.8%

4. Summary and conclusions

Real-time hybrid simulations were conducted to investigate the efficacy of a novel friction base isolator device in mitigating the effects of seismic hazards on structural systems. The device, termed the Banded Rotary Friction Device (BRFD), is a friction device based on band brake technology. An important dynamic feature of the BRFD is the self-energizing mechanism, which results in large damping forces using low-energy input. Real-time hybrid simulations are used to access the BRFD's seismic mitigation capability when placed at the base of a two-story reinforced concrete building. Seismic hazards under consideration included three MCE level near-field and three far-field earthquakes. The outcomes from the real-time hybrid simulations show that the BRFD resulted in a significant reduction in peak and residual inter-story drifts as well as reduction in structural damage.

5. Acknowledgments

The real-time hybrid simulations reported in this paper were performed at the NHERI Lehigh Experimental Facility, whose operation is supported by the National Science Foundation under Cooperative Agreement No. CMMI-2037771. Additional financial support was provided by the Pennsylvania Infrastructure Technology Alliance (PITA). Any opinions, findings, and conclusions expressed in this paper are those of the authors and do not necessarily reflect the views of the sponsors (the NSF and PITA) acknowledged herein.

6. References

ACI (American Concrete Institute). (2011). Building code requirements for structural concrete (ACI 318-11) and commentary. *American Concrete Institute*.

Ancheta, T., Darragh, R., Stewart, J., Seyhan, E., Silva, W., Chiou, B., Wooddell, K., Graves, R., Kottke, A., Boore, D., Kishida, T., & Donahue, J. (2014). NGA-West2 database. Earthquake Spectra, 30(3): 989-1005.

ASCE.(2010). Minimum design loads for buildings and other structures. *ASCE/SEI7-10*. Reston,VA.

ASCE.(2022). Minimum design loads and associated criteria for buildings and other Structures. *ASCE/SEI7-22*. Reston,VA:

Cao, L., Downey, A., Laflamme, S., Taylor, D., & Ricles, J. (2014). A novel variable friction device for natural hazard mitigation. *Proceedings of the Tenth US National Conference on Earthquake Engineering*.

Cao, L., Laflamme, S., Taylor, D., & Ricles, J. (2016). Simulations of a variable friction device for multihazard mitigation. *Journal of Structural Engineering*, 142(12), H4016001.

Cao, L., Marullo, T., Al-Subaihawi, S., Kolay, C., Amer, A., Ricles, J., Sause, R., & Kusko, C. (2020). NHERI Lehigh experimental facility with large-scale multi-directional hybrid simulation testing capabilities. *Frontiers in Built Environment*, 6(107).

Chae, Y., Kazemibidokhti, K., & Ricles, J. (2013). "Adaptive time series compensator for delay compensation of servo-hydraulic actuator systems for real-time hybrid simulation," *Earthquake Engineering and Structural Dynamics*, 42(11): 1697–1715.

Chopra, A. (2011). *Dynamics of Structures: Theory and Applications to Earthquake Engineering*. 4th Ed. Upper Saddle River (NJ): Prentice Hall Inc.

Deb, S. (2004). Seismic base isolation – an overview. *Current Science*, 1426-1430.

Downey, A., Cao, L., Laflamme, S., Taylor, D., & Ricles, J. (2016). High capacity variable friction damper based on band brake technology. *Engineering Structures*, *113*, 287-298.

Huggins, P., L. Cao, A. Downey, J. Ricles. (2023) "Research Experiences for Undergraduates (REU), NHERI 2023: Characterization and Modeling of a Semi-active Rotary Friction Damper." DesignSafe-CI. https://doi.org/10.17603/ds2-wtck-5y96 v1

Jangid, R. & Kelly, J. (2001). Base isolation for near-fault motions. *Earthquake engineering & structural dynamics*, 30(5): 691-707.

Kolay, C., & Ricles, J. (2018). Force-based frame element implementation for real-time hybrid simulation using explicit direct integration algorithms. *Journal of Structural Engineering*, 144(2), 04017191.

Kolay, C., & Ricles, J. (2019). Improved explicit integration algorithms for structural dynamic analysis with unconditional stability and controllable numerical dissipation. *Journal of Earthquake Engineering*, 23(5): 771-792.

Malik, F., & Kolay, C. (2023). Optimal parameters for tall buildings with a single viscously damped outrigger considering earthquake and wind loads. *The Structural Design of Tall and Special Buildings*, 32(7).

Montazeri, M., Namiranian, P., Pasand, A., & Aceto, L. (2023). Seismic performance of isolated buildings with friction spring damper. *Structures*, 55: 1481-1496.

Ricles, J., Kolay, C., & Marullo, T. (2020). "HyCoM-3D: A Program for 3D Multi-Hazard Nonlinear Analysis and Real-Time Hybrid Simulation of Civil Infrastructure Systems," *ATLSS Report No. 20-02*, ATLSS Engineering Research Center, Lehigh University, Bethlehem, PA.

Symans, M., Charney, F., Whittaker, A., Constantinou, M., Kircher, C., Johnson, M., & McNamara, R. (2008). Energy dissipation systems for seismic applications: current practice and recent developments. *Journal of structural engineering*, 134(1): 3-21.